# Bioinspired temperature responsive multilayer films and their performance under thermal fatigue

N. Athanasopoulos[1], N. J. Siakavellas[1]
[1]University of Patras, Department of Mechanical Engineering & Aeronautics, Patras 26500, Greece
nathan@mech.upatras.gr, nikos.athanasop@gmail.com
Tel.: +30 6946630065, Fax.: +30 2610997241

In Nature, it is common for living plants and non-living plant tissues to consist of materials with anisotropic multilayer and non-homogenous structure. The structure of tissues determines their self-shaping and self-folding capabilities in response to a stimulus in order to activate different functionalities. Predetermined movements are realized according to changes in environmental conditions, which trigger the fibrous anisotropic structure of the plants' material. In this study, we present the fabrication process of low-cost anisotropic multilayer materials that are capable of realizing complex movements caused by small temperature changes (< 40 ºC). The mismatch in the thermo-mechanical properties between three or more anisotropic thin layers creates responsive materials that alter their shape owing to the developed internal stresses. Isotropic layers can perform only bending movements, whereas anisotropic multilayer materials can perform bending, twisting or complex combined modes. The movements of the material can be controlled by forming anisotropic homogenous metallic strips over an anisotropic polymer. As a result, inexpensive responsive materials can be developed to passively react to a very broad range of thermal requirements. We studied the major parameters that affect the sensitivity of the developed materials, as well as their failure modes and crack formation under thermal fatigue conditions.

**Keywords:** Responsive materials; Smart materials; Bioinspired materials; Non-living plant tissues; Anisotropy; Thermal fatigue; Microstructure; 4D printing; Additive manufacturing

Preprints (www.preprints.org) | NOT PEER-REVIEWED | Posted: 14 June 2018 doi:10.20944/preprints201806.0227.v1

Peer-reviewed version available at Biomimetics 2018, 3, 20; doi:10.3390/biomimetics3030020

## 1. Introduction

Advances in materials' technology have the potential to greatly affect a plethora of applications in different sectors. Pressing needs to be fulfilled are the low weight structures, the integration of different functionalities and sensing abilities, as well as the energy efficiency & financial feasibility in different applications.

In Nature, extremely complex movements can be realized through the materials' self-shaping & self-folding capabilities in response to a stimulus [1-10]. Leaves/petals perform nastic movements and alter or adapt their geometrical characteristics in order to function properly using purely mechanistic strategies. Moreover, the non-living tissues of various plants are designed to undergo predetermined shape transformations through the triggering of their fibrous and multilayer micro-structure [4,5,7-10]. The coefficients of hygroscopic expansion are the corresponding parameters characterizing such changes of physical dimensions of the plants' non-living tissues [6,8-10]. Pine cones, dandelions and other non-living plant tissues transform drastically their shape using only their multilayer and anisotropic structure, Fig. 1A.

The mechanistic behaviour / transformation of the aforementioned non-living tissues can be mimicked and controlled through the use of i) multi-layered fibrous anisotropic materials or ii) anisotropic nano-composites or iii) pre-stressed sheets, or iv) nano-reinforced multilayer hydrogels [11-18]. The geometry of these materials can be transformed under temperature stimulus or humidity, while their initial and final shapes can be determined by a) the geometry, b) the homogeneous or non-homogeneous nature of the materials' structure, as well as the c) the anisotropic nature of the different layers.

The proposed responsive multilayer anisotropic materials / films are able to passively reacting under temperature stimuli by transforming from 2D to 3D complex shapes. In this study, we will present the fabrication process of low cost anisotropic multilayer films in which a temperature change generates large deformations and rotations; this behaviour is attributed to the mismatch of the coefficient of thermal expansion and the anisotropic structure of the multilayer film that causes the material's transformation. The anisotropic structure of the multilayer materials can perform bending, twisting or complex combined modes. As a result inexpensive "smart materials" can be developed to passively react to a very broad range of thermal requirements, which cannot be achieved by SMPs and SMAs [19]. These materials behave in a similar manner to 4D biomimetic materials [14] but the fabrication process can be faster and inexpensive. We present the fabrication process step by step in order to develop low cost responsive materials / films. Moreover, the current study aims to provide critical information regarding the resistance of the materials under thermal fatigue. Three different anisotropic multilayer films were tested under thermal fatigue and we investigated the types of failure and crack formation using scanning electron microscopy.

## 2. Materials and Methods

### 2.1. Structure of the material and shape transformation

The films consist of passive and responsive / active regions (black colour), Fig. 1B. The sensitivity of the film is related to the density of the strips, the coefficient of thermal expansion (CTE) of the different materials and the degree of the orientation of the polyethylene. The high mismatch of the CTE, between the polymeric layers and the metallic strips creates materials that are very sensitive in temperature and alter their shape drastically owing to the developed internal stresses and their anisotropic nature. The deformable regions are very responsive to temperature, presenting extremely large deformations. The spatial distribution of these strips and their direction, determine the shape of the film as a function of temperature. Therefore, the pattern of the strips, the thickness and the thermo-mechanical properties of the various materials determine the entire geometry transformation, thus enabling their a priori design.

The multilayer structure of the film differs for each region; however, the following layers must be combined to achieve proper function: one anisotropic low-CTE layer (strips), one high-CTE

anisotropic layer (polyethylene), and one layer of adhesive. Moreover, we can incorporate more layers in order to achieve higher deformation and better thermal fatigue performance.

Figure 1B presents the response of a film that has been designed to be transformed to a helix. In this case, the principal axes of the oriented polyethylene and the aluminum strips are coincides in a 45° direction. The maximum temperature is approximately T ≈ 55 °C. Supplementary Videos S1, S2 and S3 present the transformation of multilayer films with different anisotropic properties and geometries.

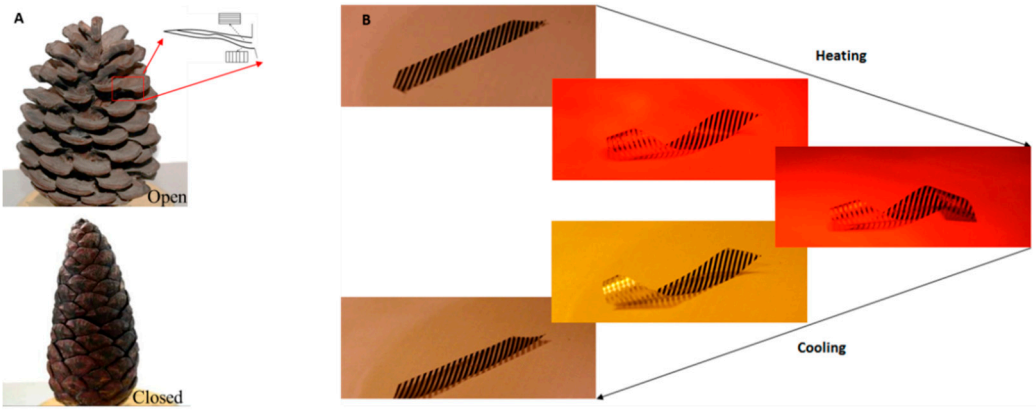


**Figure 1. (A)** Pine cone and its multilayer structure, **(B)** Response of the developed anisotropic film during heating and cooling stage.

## 2.2. Fabrication process

A two-component adhesive for low surface energy plastics (Methacrylat- and Amine-based resins) was used and applied on the oriented polyethylene (PE), Fig 2A. It must be mentioned that any adhesive for low surface energy plastics can be used. The mask was attached over an aluminum film under pressure using hot rolling press at 180 °C in order to form the strips at the desired directions, Fig 2B. The masked aluminium film was pressed together with the bilayer material using cold rolling press, Fig. 2C. Then, the aluminium strips were formed using a chemical etching technique through ferric chloride solution at 40 °C for < 20 min. The final formed multilayer materials were cleaned and removed from the flat tool using acetone, Fig. 2D.

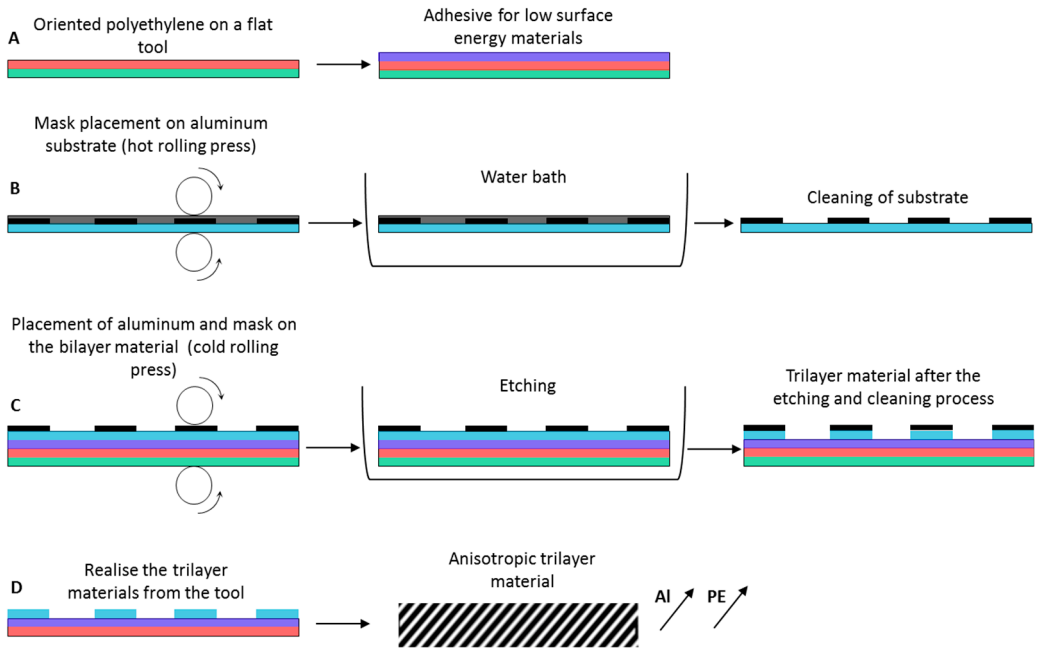


**Figure 2.** Fabrication process of the bioinspired films / materials. **(A)** Fabrication of the bilayer material over a flat tool, **(B)** mask placement over the aluminum film using hot roll press and cleaning, **(C)** cold roll pressing of the different layers and strips' formation using etching techniques, **(D)** cleaning and demoulding.

This fabrication process can be used for the continuous production of small or large surfaces with different thicknesses and can be adopted for the fabrication of inexpensive responsive materials.

### 2.3. Anisotropic multilayer films - Specimens

The sequence of the anisotropic layers and the strips of the passive and responsive / active regions that were used are presented in Fig. 3. Three different films were developed and tested. A) The first multilayer material consists of aluminum strips (thickness ≈ 5μm) over a bilayer material (41μm polyethylene and adhesive). B) The second multilayer film consists of aluminum strips (thickness =18μm) over the same bilayer material. The third multilayer material consists of aluminum strips (thickness =18μm) over a trilayer material (41μm polyethylene, adhesive, 18μm aluminum film).

The multilayer materials were tested under thermal cycling fatigue measuring their deflection before and after the N thermal cycles. The failure modes were examined using scanning electron microscope (SEM).

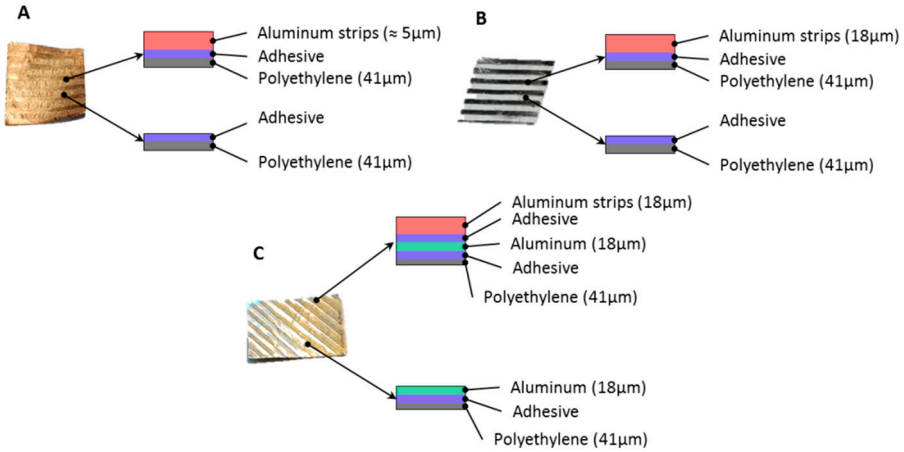


**Figure 3.** Test specimens for SEM characterization (10 mm x 10 mm). **(A)** Aluminum strips over a bilayer material (Aluminum thickness = 5μm), **(B)** Aluminum strips over a bilayer material (Aluminum thickness = 18μm), **(C)** Aluminum strips over a trilayer material (Aluminum thickness = 18μm).

## 3. Results and discussion

We studied the response of different anisotropic multilayer films and how their geometry has been affected by the degradation of the mechanical properties due to the fast thermal fatigue conditions. Through the aforementioned experimental methodology, we intended to examine the performance of the films and identify the failure modes of the material. Figure 4A presents the dimensions of the specimens and their geometry. During the heating stage of the thermal fatigue test, the film is bended as Fig. 4B depicts.

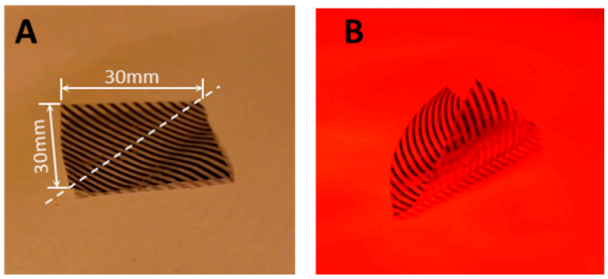


**Figure 4. (A)** Dimensions of the specimens and shape at ≈ 20 ºC, **(B)** Bending of the film under infrared heating (IR lamp) at ≈ 55 ºC.

Preprints (www.preprints.org) | NOT PEER-REVIEWED | Posted: 14 June 2018 doi:10.20944/preprints201806.0227.v1

Peer-reviewed version available at Biomimetics 2018, 3, 20; doi:10.3390/biomimetics3030020

### 3.1. Thermal cycling fatigue

The scope of this experimental procedure is to evaluate the performance of the bioinspired film under accelerated thermal fatigue. An experimental setup was developed to study the degradation of the mechanical properties and the shape-shifting of the film. During the transformation of the material, any degradation in the polymeric layers would result to a different shape. Moreover, any failure of the layers or any interlaminar failure between the strips and the substrate (polyethylene) would result to the shape shift of the film.

The experimental setup consisted of an IR lamp, a fan, a digital timer and counter, a power supply, a laser distance meter (micro-epsilon CS3), a reflector curtain, and the tested anisotropic multilayer film, Fig. 5B. The digital timer controlled the operation time of the IR lamp and that of the fan. The IR lamp heated the film until it reached its final-transformation position. Immediately after the heating phase, the film was cooled using a fan as a cooler and it returned to its initial position. A laser measurement device was continuously recording the distance of a constant point (from A to B, Fig. 5B) during the cooling phase. Any change in the recorded distance during cooling or any change in the measured distance of the initial position (A) or final position (B) would indicate that the mechanical properties of the multilayer material have been degraded or that a failure has occurred.

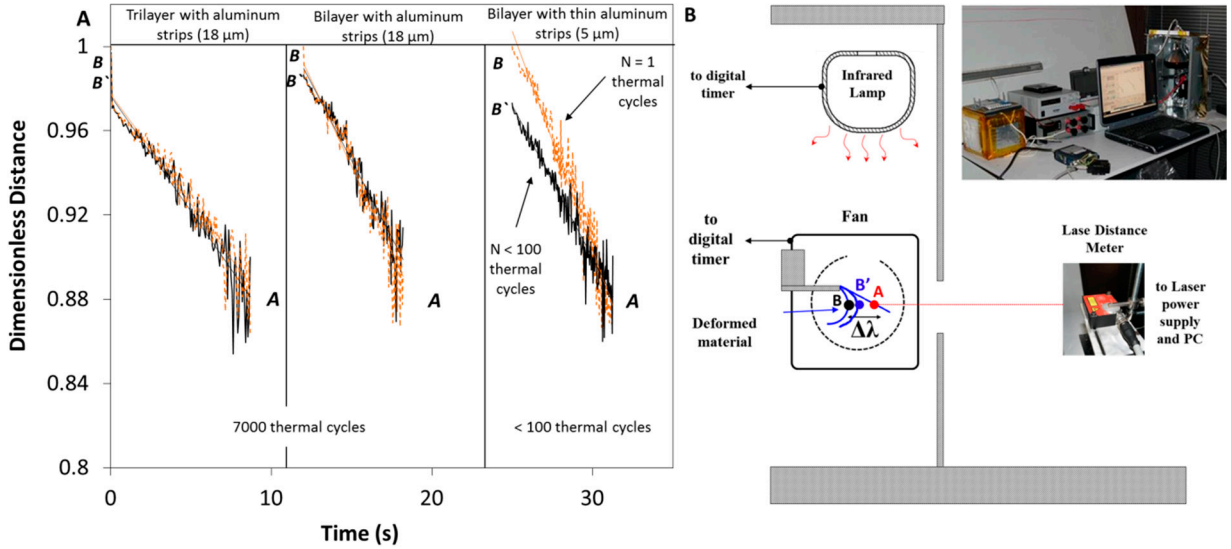


**Figure 5. (A)** Distance measurement of the position of point B to point A during the cooling stage after N thermal cycles, **(B)** Apparatus of the thermal fatigue test.

Figure 5A presents the measured distance versus time at the cooling phase after a certain number of thermal cycles for the three different developed films. The orange line represents the measured distance of the film during its first response (1st thermal cycle), whereas the black line represents the recorded distance of the film (point B to point A) after a certain number of thermal cycles (Nth thermal cycle).

**Film 3: 18μm aluminum strips on a trilayer film with aluminum substrate:** any change in the final position of the measured point (point B to point B`, Fig. 5B) was indicative of the fact that the mechanical properties of the multilayer material were degraded and that the shape of the film changes. For the 3rd specimen, the distance between the location of the final position (Fig. 5A, 1st column) at the beginning of the test and at the end of the test (after 7,000 thermal cycles) changed by $B_{N=1} - B`_{N=7000} = 0.3$ mm.

**Film 2: 18μm aluminum strips on polymeric substrate:** the distance between the location of the final position (Fig. 5A, 2nd column) of the second specimen during the beginning and the end of the test (after 7,000 thermal cycles) changed by $B_{N=1} - B`_{N=7000} = 1.3$ mm. Moreover, we observe that the inclination of the curve of the measured distance versus time at the beginning of the test and after 7,000 thermal cycles remains approximately similar, Fig. 5A. The multilayer film became

Preprints (www.preprints.org) | NOT PEER-REVIEWED | Posted: 14 June 2018 doi:10.20944/preprints201806.0227.v1

Peer-reviewed version available at Biomimetics 2018, 3, 20; doi:10.3390/biomimetics3030020

more rigid and its response to temperature was less sensitive due to the hardening of the polymeric layers. The sensitivity of the film is different and smaller than the sensitivity at the beginning of the experiment. The hardening of the material is also related to the heating and cooling rate; therefore, smaller rates would lead to smaller shape shifts because of the materials degradation. The tested films after 7,000 thermal cycles were still healthy and no significant failure was occurred. Despite the very good performance of the multilayer material, we observed that local degradation may occur because of material imperfections and inaccuracies in the manufacturing process.

**Film 3: 5μm aluminum strips on polymeric substrate:** In contrast, the distance between the locations of the final position (point B to point B`, Fig. 5B) of the 1st specimen at the beginning of the test and at the end of the test, for less than 100 thermal cycles, changed by $B_{N=1} - B`_{N=7000} = 2.8$ mm. As a result, the inclination of the curve of the measured distance versus time at the beginning of the test and at 100 thermal cycles changes significantly (Fig. 5A, 3rd column). Extensive cracks were observed and as a result the response of the multilayer material was decreased.

### 3.2. Surface and crack formation characterization through SEM

Three different specimens were examined through SEM (Scanning Electron Microscope, JEOL 6300). Each specimen was examined before and after the thermal cycling test.

#### 3.2.1. Film 1: 5μm aluminum strips on polymeric substrate – 1st specimen

Figure 6A presents the transformed shape of the anisotropic film. The thickness of the aluminum strips is approximately 5μm. Figures 6B and 6C present the aluminum strips and the occurred failures in different magnification, after few thermal cycles (N < 100). The small thickness of the strips and their large deformation create small interlaminar failures. After a few thermal cycles, extensive failures are observed because of the compressive forces. Consequently, the interlaminar failures of the strips create extensive cracks on the entire material. The crack formation occurs due to buckling effects on the thin aluminum strips, Fig. 6D. The observed crack pattern is very similar to the mud-crack patterns.

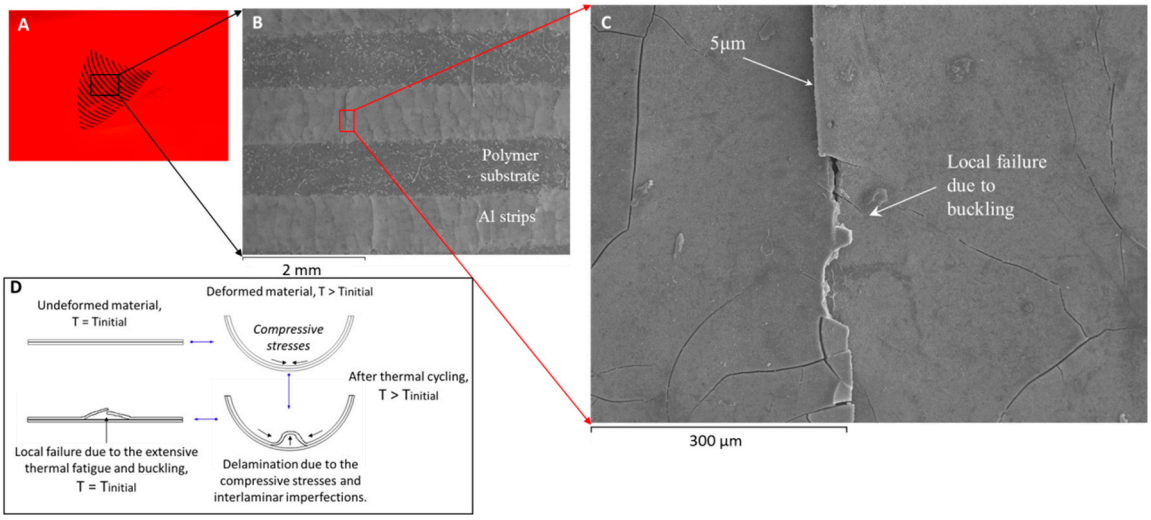


**Figure 6. (A)** Film and **(B, C)** surface characterization of the 1st film after few hundreds of thermal cycles (strips with 5μm thickness), **(D)** crack formation. The temperature change was 35 °C

As the width of the strips decreases the direction of the cracks will be perpendicular to the direction of the strip. On the other hand, as the width of the strips increases the crack formation pattern will be very similar to the mud-crack formation. Despite the extensive crack formation the material remains functional and is capable of achieving large deformations. However, the sensitivity of the film was decreased significantly.

Preprints (www.preprints.org) | NOT PEER-REVIEWED | Posted: 14 June 2018 doi:10.20944/preprints201806.0227.v1

Peer-reviewed version available at Biomimetics 2018, 3, 20; doi:10.3390/biomimetics3030020

### 3.2.2. Film 2: 18μm aluminum strips on polymeric substrate – 2nd specimen

Figure 7A presents the formed aluminum strips of the health material on the polyethylene layer. The thickness of the aluminum film is 18μm. We did not observe any delamination or crack prior to the thermal cycling test, Fig. 7B. Only small defects exist due to manufacturing inaccuracies. After 7,000 thermal cycles, the material remains functional without significant loss in its performance, Fig. 7C. Small delaminations (interlaminar failures) observed at the edges of the strips, Fig. 7C, D due to the poor adhesion of the strips with the polyethylene. These small delaminated regions have been initiated due to the compressive stresses, as well as the small imperfections. However, in a specimen with dimensions 10 mm by 10mm, we did not observe any crack. Moreover, only 5 interlaminar failures were observed.

These interlaminar failures can be eliminated if we increase the width of the strips. Also, the delaminated regions could be decreased with the addition of an extra aluminum layer between the strips and the polyethylene. In this case the shear strength of the adhesion between the strips and the substrate is significantly higher.

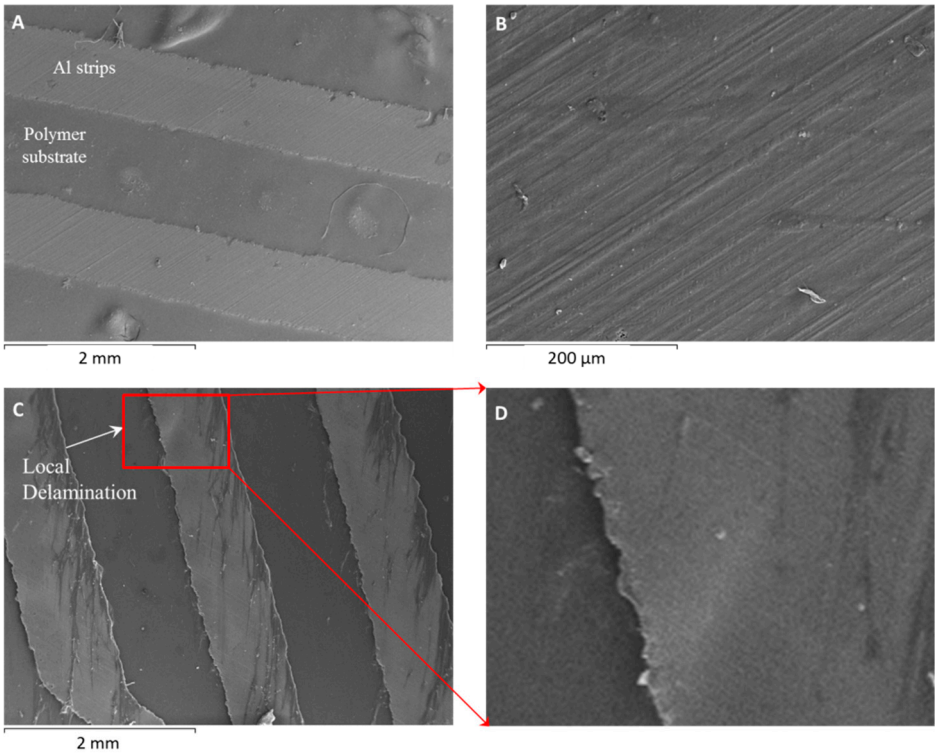


**Figure 7.** SEM images of the **(A)** aluminum strips over polymeric substrate and **(B)** morphology of the aluminum strips' surface before the thermal fatigue. SEM images of the **(C)** aluminum strips over polymeric substrate and **(D)** edge delamination of the aluminum strip after 7000 thermal cycles. The temperature change was ≈ 45 °C

### 3.2.3. Film 3: 18μm aluminum strips on a trilayer film with aluminum substrate

In addition, a different film was developed in order to characterize its performance and any possible failure. In this case, the aluminum strips have been adhered on an aluminum substrate and not directly on the polyethylene's surface.

Figure 8A presents the formed aluminum strips of the health material on the aluminum layer. The thickness of the aluminum film as well as the thickness of the aluminum strips is 18μm. We did not observe any delamination or crack prior to the thermal cycling test, Fig. 8A-C. Similarly, small defects exist due to manufacturing inaccuracies. After 7000 thermal cycles, the material remains functional without significant loss in its performance. Small delaminations observed at the edges of the strips due to the compressive forces. However, in a specimen with dimensions 10 mm by 10mm, we did not observe any crack. Approximately, only two delaminated regions were observed, Fig. 8D, E.

Preprints (www.preprints.org) | NOT PEER-REVIEWED | Posted: 14 June 2018 doi:10.20944/preprints201806.0227.v1

Peer-reviewed version available at Biomimetics 2018, 3, 20; doi:10.3390/biomimetics3030020

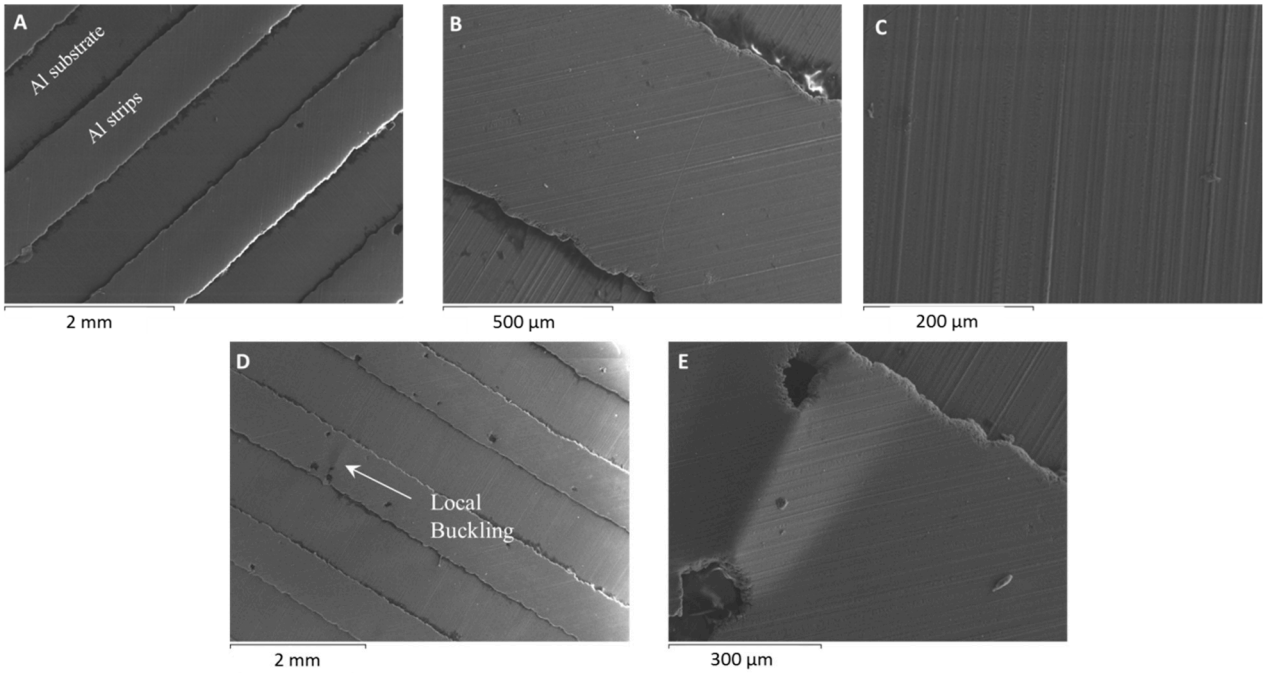


**Figure 8.** SEM images of the **(A)** aluminum strips over aluminum substrate and **(B, C)** morphology of the aluminum strips' surface before the thermal fatigue. SEM images of the **(D)** aluminum strips over aluminum substrate and **(E)** edge delamination of the aluminum strip after 7000 thermal cycles. The temperature change was ≈ 45 ºC

The material remains functional after 7,000 thermal cycles and is capable of achieving large deformations keeping its exact geometry, during the heating or cooling stage, Fig. 5A.

## 4. Conclusions

Dead tissues alter drastically their geometry using only their multilayer and anisotropic fibrous structure. Similarly, complex movements and large deformations in response to a stimulus can be realized using common/commercial multilayer, anisotropic and homogeneous or non-homogeneous materials. The shape shifting of the material can be triggered under temperature stimulus. The spatial distribution of the strips on the polyethylene surface determines the manner in which they transform their structure. Controlling the direction and the distribution of the strips we can design a material to form a circle or a helix or more complex shapes.

The resistance of the bioinspired films in thermal cycling is strongly related to the thickness of the strip, as well as the type of the substrate. Very thin aluminum strips cannot withstand the excessive thermal fatigue due to the compression forces. Small imperfections and poor adhesion initiate small delaminations and buckling failures after a few thermal cycles. In contrast, thicker aluminum strips present excellent resistance in thermal fatigue after a few thousands of thermal cycles.

The proposed responsive multilayer anisotropic materials / films will create opportunities and actively strengthen the development of low cost smart materials, leading to their commercialization in different sectors, such as the building sector [20, 21], sensors, transformable electronics, soft robotics [13], light control [18], passive thermoregulation in Space applications [17] and additive manufacturing in general [13, 14].

## Supplementary Material

**Video S1:** Bending movement at 0deg direction (Speed x 4).
**Video S2:** Bending movement at 45deg direction (Speed x 4).
**Video S3:** Transformation of a flat strip to helix (Speed x4).

**Acknowledgments**

This research is conducted through the IKY scholarships program, and is co-financed by the European Union (European Social Fund - ESF) and the Greek national funds through the action entitled "Reinforcement of Postdoctoral Researchers" of the National Strategic Reference Framework (NSRF), 2014–2020.

Moreover, we would like to thank the Laboratory of Electron Microscopy and Microanalysis (L.E.M.M.) of University of Patras for the provided services and assistance.

**Author Contributions** The manuscript was written by both authors. The central idea and the problem were conceived and formulated by N.A. N.A. and N.J.S designed the testing setup, analyse the results and conduct the experiments. All the materials have been developed by N. A.

**Competing financial interests**

The author(s) declare no competing financial interests.

**References**

1. Tao, P.; Shang, W.; Song, C.; Shen, Q.; Zhang, F.; Luo, Z.; Yi, N.; Zhang, D.; Deng, T. Bioinspired engineering of thermal materials. Adv. Mater. **2015**, 27, 428–463.
2. Nilsen, E.T. Why Do Rhododendron Leaves Curl. Journal American Rhododendron Society 40, **1986**, 31–35.
3. Ye, C.; Li, M.; Hu, J.; Cheng, Q.; Jiang, L.; Song, Y. Highly reflective superhydrophobic white coating inspired by poplar leaf hairs toward an effective 'cool roof'. Energy Environ. Sci. **2011**, 4, 3364.
4. Dawson, C.; Vincent, J. F. V.; Rocca, A.-M.; How pine cones open. **1997**, Nat. 390**,** 668.
5. Forterre, Y. Slow, fast and furious: Understanding the physics of plant movements. *J. Exp. Bot.* **2013**, 64, 4745–4760.
6. Schleicher, S.; Lienhard, J.; Poppinga, S.; Speck, T.; Knippers, J. A methodology for transferring principles of plant movements to elastic systems in architecture. *CAD Comput.* **2015** *Aided Des.* 60, 105–117.
7. Audoly, B.; Pomeau, Y. Elasticity and Geometry. **2010**, *Oxford university press.*
8. Reyssat, E.; Mahadevan, L. Hygromorphs: from pine cones to biomimetic bilayers. *J. R. Soc Interface,* **2009,** 6(39), 951–957.
9. Holstov, A.; Farmer, G.; Bridgens, B. Sustainable Materialisation of Responsive Architecture. *Sustainability,* **2017**, 9(3), 435.
10. Bertinetti, L.; Fischer, F.D.; Fratzl, P. Physicochemical Basis for Water-Actuated Movement and Stress Generation in Nonliving Plant Tissues. *Phys. Rev. Lett.* **2013,** 238001.
11. Athanasopoulos, N.; Siakavellas, N. J. Programmable thermal emissivity structures based on bioinspired self-shape materials. *Sci. Rep.* **2015**, 5, 17682.
12. Andres, C.M.; Zhu, J.; Shyu, T.; Flynn, C.; Kotov, N.A. Shape-morphing nanocomposite origami. *Langmuir* **2014**, 30, 5378–5385.
13. Momeni, F.; Mehdi Hassani, N,S.; Liu, X.; Ni, J. A review of 4D printing. *Mater. Des.* **2017,** 122, 42–79.
14. Gladman, S.; Matsumoto, A.; Nuzzo, E.A.; Mahadevan, L.; & Lewis, J.A. Biomimetic 4D printing. *Nat. Mater.* **2016**, 15, 413–418.
15. Erb, R.M.; Sander, J.S.; Grisch, R.; Studart, A.R. Self-shaping composites with programmable bioinspired microstructures. *Nat. Commun.* **2013**, 4, 1712.
16. Zhao, Q.; Zou, W.; Luo, Y.; Xie, T. Shape memory polymer network with thermally distinct elasticity and plasticity. *Science Advances,* **2016**, 2(1), e1501297.
17. Athanasopoulos, N.; Siakavellas, N.J. Smart patterned surfaces with programmable thermal emissivity and their design through combinatorial strategies. *Sci. Rep.* **2017**, 7, 12908.

18. Athanasopoulos, N.; Siakavellas, N.J. Self-shape structures with programmable thermal radiative properties. *Conference: Multifunctional Materials & Structures / Gordon Research, Ventura, California,* **2016**, poster ordinal 3rd.
19. Hawkes, E.; An, B.; Benbernou, N.M.; Tanaka, H.; Kim, S.; Demaine, E.D.; Rus, D.; Wood, R.J. Programmable matter by folding. *Proc. Natl. Acad. Sci.* **2010**, 107, 12441–12445.
20. Fiorito, F.; Sauchelli, M.; Arroyo, D.; Pesenti, M.; Imperadori, M.; Masera, G.; Ranzi, G.Shape morphing solar shadings: A review. Renew. Sustain. Energy Rev. **2016**, 55, 863–884.
21. Khoo, C.; Salim, F.; Burry, J. Designing Architectural Morphing Skins with Elastic Modular Systems. *Int. J. Archit. Comput.* **2011,** 9, 397–420.